^{207}Pb-^{206}Pb GEOCHRONOLOGY AND MICROSTRUCTURES OF PHOSPHATES FROM APOLLO 14 AND 15 SOILS. C. A. Crow[1], T. M. Erickson[2], R. Economos[3], K. Lehman Franco[3], J. W. Boyce[2], J. R. Davis[1], C. A. Diaz[1], R. M. Flowers[1], M. J. Brounce[4], B. Schoene[5]. [1]University of Colorado Boulder (carolyn.crow@colorado.edu), [2]Jacobs Technology/NASA Johnson Space Center, [3]Southern Methodist University, [4]University of California, Riverside, [5]Princeton University.

Introduction: Phosphates (apatite and merrillite) are common accessory minerals in many Apollo basalt and regolith samples. Phosphates typically have lower closure temperatures than their companion accessory phase zircon for their U-Pb and (U-Th)/He geochronologic systems [e.g., 1, 2]. As such, the ages of phosphates in impact melt-bearing breccias have typically been used to constrain the ages of impact events [3]. Phosphates have also served as anchors for ^{207}Pb-^{206}Pb isochrons allowing for precise ages of basaltic samples to be determined [4]. Apatite is also a reservoir for volatile species (e.g., F, Cl, OH, S) [e.g., 5, 6] which are important for investigating the formation and evolution of the lunar interior [7-11]. Recent work by [11] and [12] has shown that deformation and exposure to high temperatures, especially those in impact environments, can influence both apatite chronology and chemistry. Here we present the first chronology and microstructure results of a large consortium study aimed at unraveling the impact and endogenous volatile record of phosphates extracted from lunar soils. These soils potentially sample a larger range of lithologies than the rocks returned by Apollo astronauts, and should, therefore, represent a more global phosphate record. For more information on low-temperature (U-Th)/He thermochronology, please see the companion abstract [13].

Samples: Phosphates were isolated from two Apollo 14 soils (14163 and 14259) and one Apollo 15 soil (15311), which were previously processed by [14, 15] for extraction of zircon grains using methylene iodide density separation. Sample 14163 is a submature sample collected from a small (2-foot crater) [16]. Sample 14259 is considered complementary to 14163 because it was collected from the top 1 cm of the surface and has a high maturity index [16, 17]. Sample 15311 is a rake sample collected near the edge of Spur Crater and is a companion of soil 15301, which is submature [16].

Methods: The heavy liquid floats from [14,15] were further magnetically separated using a neodymium hand magnet. The non-magnetic fraction, typically much less than 1% of the sample, were sprinkled on Kapton tape and mapped using EDS (Energy Dispersive Spectroscopy) with the JEOL IT500HR field emission SEM (Scanning Electron Microscopy) at Southern Methodist University. Identified phosphates were then mounted in epoxy pucks for subsequent analytical work.

Electron Backscatter Diffraction (EBSD). EBSD analyses were collected using a JEOL 7900F field emission Scanning Electron Microscopy with an Oxford Instruments Symmetry detector at NASA Johnson Space Center. Analytical conditions included a 20 KV accelerating voltage, 10 nA beam current and 20 mm working distance. Electron diffraction patterns were indexed with a fluorapatite match unit after [18] and merrillite after [19]. The data were processed using AztecCrystal.

Phosphate Compositions: Phosphate compositions were measured by wavelength dispersive x-ray spectrometry (WDS) with the JEOL 8230 Superprobe at the University of Colorado Boulder.

SIMS ^{207}Pb-^{206}Pb Geochronology: Pb-isotopes were measured during two sessions with the Cameca ims1290 at the University of California, Los Angeles using the Hyperion II ion source with an O^{-3} primary beam. Spot sizes were typically ~10 mm.

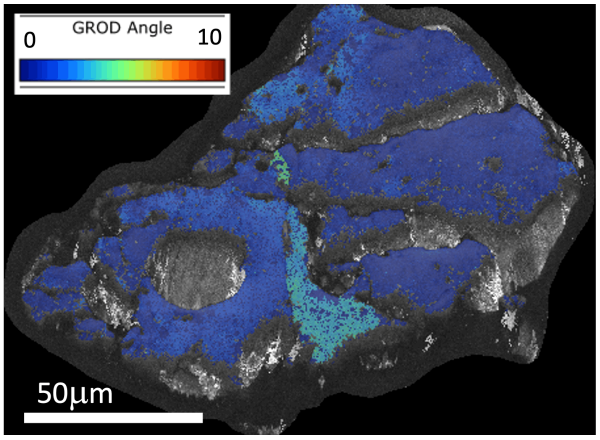

Figure 1: Lunar apatite 15311,20 #32 showing up to 5° of crystal plastic deformation (CPD). While CPD in apatite can be observed in tectonic settings on Earth, the main driver of tectonics on the Moon is impact cratering.

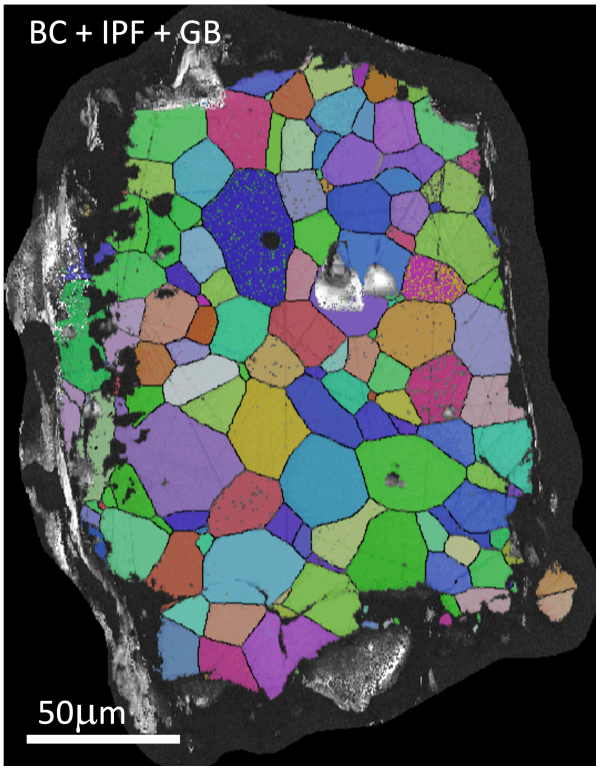

Figure 2: Lunar apatite 14259,664 #46 exhibiting granular texture suggesting post formation recrystallization.

Results and Discussion: To date, we have coordinated compositions, microstructures, and geochronology for 32 phosphates from 14259, nine from 14162, and seven from 15311. [Note: this reflects the number of grains for which all three datasets have been collected]. ESBD and compositional data has been collected for a larger suite of grains. The phosphates are primarily fluorapatite and merrillite with a few unusual high-Si phosphates.

The EBSD results show a range of textures from crystalline grains with minimal deformation, to crystal-plastically deformed grains (Fig. 1), to grains composed of strain free polygonal neoblasts with triple-junctions indicative of higher temperature and pressure metamorphism and complete thermal annealing (Fig. 2).

The Pb-isotopes of the phosphates show a range of inherited or common Pb contributions. There are eight phosphates with $^{204}Pb/^{206}Pb$ ratios less than 10^{-4} for which common Pb-corrections will have a negligible influence on calculated $^{206}Pb/^{207}Pb$ ages. Seven of these grains have ages of ~3.9 Ga, which is a common age for lunar phosphates [20,21]. However, one grain from 15311 has a noticeably older age of ~4.2 Ga. Ongoing Pb-isotope analyses will help us further constrain the ages of phosphates with appreciable ^{204}Pb [Katelyn?].

In this presentation, we will synthesize the microstructural and ^{207}Pb-^{206}Pb geochronology to better interpret the significance of the ages and to compare with the phosphate record from rock samples from Apollo 14 and 15 landing sites, together with other lunar return samples [23] and meteorite materials [24].

Acknowledgments: We would like to thank AARB and the NASA Curation Office for access to the samples used in this study. This work is supported by NASA Solar Systems Workings Grant # 80NSSC0K0148.

References:

[1] Flowers R. M. et al. (2009) *GCA, 73,* 2347-2365. [2] Schoene B. and Bowring S. A. (2007) *GCA, 71,* 165-185. [3] Nemchin A. A. et al. (2010) *MAPS, 44,* 1717-1734. [4] Snape J. F. et al. (2018) *Chem. Geol., 482,* 101-112. [5] MuCubbin F. M. et al. (2010) *Nat. Acad. Sci., 107,* 11223-11228. [6] Boyce J. W. et al. (2010) *Nature, 446,* 466-469. [7] Taylor S. R. et al. (2006) *Rev. Min. Pet., 60*, 657-704. [8] Hui. H. et al. (2013) *Nat. Geoscience*, 6, 177-180. [9] Ni P. et al. (2019) *GCA*, *249,* 17-41. [10] Lin Y. et al. (2019) *Geoch. Persp. Let., 10*, 14-19. [11] Boyce J. W. et al. (2018) *LPSC XLIX*, A#2492. [12] Černok A. et al. (2018) *MAPS, 54,* 1262-1282. [13] Diaz C. A. et al. *This Conference.* [14] Crow C. A. et al. (2018) *GCA, 202*, 264-284. [15] Taylor D. J., Mckeegan K. D., & Harrison T. M. (2019) *EPSL, 279,* 157-164. [16] Morris R. V. (1978) *9th LSC*, 2287-2297. [17] Moore C. B. et al. (1972) *3rd LSC,* 2051-2058. [18] Comodi et al. (2001) *Phys. Chem. Min*., *28,* 219-224. [19] Xie et al. (2015) *Am. Min., 100,* 2753-2756. [20] Nemchin A. A. et al. (2021) *Geochem.*, 18, 125683. [21] Merle R. E. et al. (2014) *MAPS, 49,* 2241-2251. [22] Lehman Franco K. et al. *This Conference*. [23] Thiessen F.K. (2018) *Doctoral dissertation, Department of Geological Sciences, Stockholm University*. [24] Curran N. M. et al. (2019) *MAPS, 54*, 1401-1430.